

Pulsar Spindown by a Fall-Back Disk and the $P - \dot{P}$ Diagram

M. Ali Alpar

*Faculty of Engineering and Natural Science, Sabanci University,
Orhanli-Tuzla, Istanbul 81474, Turkey*

Aşkin Ankay and Efe Yazgan

Department of Physics, Middle East Technical University, Ankara 06531, Turkey

ABSTRACT

Neutron stars may be surrounded by fall-back disks formed from supernova core-collapse. If the disk circumscribes the light-cylinder, the neutron star will be an active radio pulsar spinning down under the propeller spin-down torque applied by the disk as well as the usual magnetic dipole radiation torque. Evolution across the $P - \dot{P}$ diagram is very rapid when pulsar spin-down is dominated by the propeller torque. This explains the distribution of pulsars in the $P - \dot{P}$ diagram.

Subject headings: stars: neutron, pulsars

1. Introduction

Recent efforts to understand the nature of several newly identified classes of neutron stars, in particular anomalous X-ray pulsars (AXPs - Mereghetti 1999) and soft gamma-ray repeaters (SGRs) (Woods et al. 1999) have followed two avenues. Magnetar models, involving neutron star dipole magnetic fields $B \sim 10^{14} - 10^{15}$ G, above the quantum critical field $B_c = m^2 c^3 / e\hbar = 4.4 \times 10^{13}$ G, were advanced to explain the mechanism and energetics of soft gamma-ray repeaters particularly (Thompson & Duncan 1995). The alternative models propose to explain the new classes of neutron stars in terms of conventional $B \sim 10^{12}$ G fields. These alternative models involve accretion or propeller (Illarionov & Sunyaev 1975) torques from an accretion disk surrounding the isolated neutron stars (Alpar 1999, 2001; Chatterjee, Hernquist & Narayan 2000). Alpar (1999, 2001) argued that four classes of neutron stars, radio pulsars, dim thermal neutron stars (DTNs; Treves et al. 2000), AXPs and radio quiet neutron stars (RQNSs; Chakrabarty et al. 2001) and perhaps SGRs represent alternative

pathways of young neutron stars, distinguished by the history of mass inflow (\dot{M}) from a fall-back accretion disk. This work classified young neutron stars according to ranges of \dot{M} , taken as representative constant values, with radio pulsars corresponding to zero or very weak \dot{M} , such that the disk does not quench the pulsar magnetosphere. The inner radius of the disk must lie at or beyond the light cylinder. Disks around radio pulsars were first proposed by Michel & Dessler (1981, 1983) and Michel (1988). Chatterjee, Hernquist & Narayan (2000) studied a fall-back disk with a specific time dependent mass-inflow rate $\dot{M}(t)$ taken to follow a self-similar thin disk solution, which entails a power-law decay of $\dot{M}(t)$ (Cannizzo, Lee & Goodman 1990, Mineshige, Nomoto & Shigeyama 1993). Chatterjee, Hernquist & Narayan apply this model to the AXPs in particular. According to their model some neutron stars go through propeller and accretion (AXP) phases as $\dot{M}(t)$ evolves while others, at magnetic fields $< 3 \times 10^{12} G$ become radio pulsars after a very brief initial accretion phase.

The implications of a fall-back disk for young radio pulsars are of great interest. Marsden, Lingenfelter and Rothschild (2001a,b) have argued that the presence of a propeller spin-down torque from a fall-back disk in conjunction with the magnetic dipole radiation torque may explain the large discrepancy (Gaensler & Frail 2000) between the real (kinematic) age and the characteristic age corresponding to pure dipole spin-down for the pulsar B1757-24, and that pulsar-SNR age discrepancies can be explained in a similar way. Menou, Perna and Hernquist (2001b) have invoked the propeller spin-down torque from a fall-back disk in conjunction with the magnetic dipole torque to explain the braking indices $n < 3$ of five young pulsars. In this letter we apply the combined spin-down torque, using the simple model of Menou, Perna and Hernquist (2001b), to the distribution of pulsars in the $P - \dot{P}$ diagram. Presence of torques other than the dipole radiation torques, in particular torques that might arise from the ambient medium near a young pulsar in a supernova remnant was proposed first by Yusifov et al. (1995) to explain qualitatively the measured braking indices $n < 3$ of young pulsars, the discrepancy between real and "characteristic" ages and the distribution of pulsars in the $P - \dot{P}$ diagram. Gvaramadze (2001) invokes torques from circumstellar clumps in the SNR to derive a "true" age for PSR B1509-58 in agreement with the SNR age.

In Section 2, we shall explore the combined torque model, using the canonical magnetic dipole torque together with the simple model of Menou, Perna and Hernquist (2001b) for the propeller spin-down torque, using a constant mass inflow rate \dot{M} . Evolutionary tracks in the $P - \dot{P}$ diagram will be presented in Section 3 along with analytical expressions for timespans of various phases, braking indices and other properties of the tracks. The $P - \dot{P}$ diagram is divided into strips delineated by tracks of constant magnetic field and mass inflow rate. Each strip is divided into period bins and a histogram is constructed for the number of pulsars in each period bin. A curve for the expected number of pulsars as a function of

period is calculated according to the model and compared with the histogram for each strip. The results are discussed in Section 4.

2. Spin-Down of a Pulsar with a Fall-Back Disk

We model spin-down of a pulsar under the combined action of magnetic dipole radiation and propeller spin-down torques as

$$I\Omega\dot{\Omega} = -\beta\Omega^4 - \gamma \quad (1)$$

adopting the model of Menou, Perna and Hernquist (2001b) for the propeller torque, with their notation. The neutron star will continue to act as a radio pulsar as long as the fall-back disk does not protrude into the light cylinder. If the disk were detached from the light cylinder, it would not exert any torque on the neutron star and its magnetosphere. Assuming that the inner radius of the disk is attached to the light cylinder, the torque can be estimated as:

$$N_{disk} = -2\dot{M}r_{lc}^2[\Omega - \Omega_K(r_{lc})] \cong -2\dot{M}r_{lc}^2\Omega = -2\dot{M}c^2/\Omega \equiv -\gamma/\Omega \quad (2)$$

where \dot{M} is the mass inflow rate interacting with the light cylinder and being ejected from the disk; $r_{lc} = c/\Omega$ is the light cylinder radius, and $r_{lc}^2\Omega$ is the specific angular momentum extracted from the pulsar magnetosphere, since the Keplerian rotation rate $\Omega_K(r_{lc})$ in the disk is small compared to the rotation rate Ω of the neutron star and its magnetosphere. The last equation above defines the parameter

$$\gamma = 2\dot{M}c^2 = 2 \times 10^{31}\dot{M}_{10} \text{ erg/s} \quad (3)$$

which is the rate of energy loss of the neutron star due to the propeller torque; \dot{M}_{10} is the mass inflow rate in units of 10^{10} gm/s. The rate of energy loss due to magnetic dipole radiation is given by

$$\dot{E}_{dipole} = -B_{\perp}^2 R^6 \Omega^4 / 6c^3 = -\beta\Omega^4. \quad (4)$$

Here B_{\perp} is the component of the dipole magnetic field at the neutron star surface in the direction perpendicular to the rotation axis and R is the neutron star radius. This defines

$$\beta = 6.17 \times 10^{27} B_{\perp,12}^2 R_6^6. \quad (5)$$

Menou, Perna and Hernquist (2001b) give the solution of equation (1) for constant \dot{M} as

$$\begin{aligned} t &= \tau [\arctan((\beta/\gamma)^{1/2}\Omega_i^2) - \arctan((\beta/\gamma)^{1/2}\Omega(t)^2)] \\ &= \tau [\pi/2 - \arctan((\beta/\gamma)^{1/2}\Omega(t)^2)] \end{aligned} \quad (6)$$

where Ω_i , the initial rotation rate of the pulsar, is always large enough to justify the second equation; $\Omega(t)$ is the rotation rate at time t , and the timescale τ is:

$$\tau = I/2(\gamma\beta)^{1/2} = 4.5 \times 10^7 \dot{M}_{10}^{-1/2} B_{\perp,12}^{-1} \text{ yrs} \quad (7)$$

where I denotes the moment of inertia of the neutron star. In the $P - \dot{P}$ diagram pulsars will follow tracks given by Equation (1),

$$\dot{P} = (4\pi^2\beta/I)P^{-1} + (\gamma/4\pi^2I)P^3. \quad (8)$$

Menou, Perna and Hernquist (2001b) have used this model to explain the observed values of the braking index

$$n = \ddot{\Omega}\Omega/\dot{\Omega}^2 \quad (9)$$

for PSR B0531+21 (Crab), PSR B0540-69, PSR B0833-45 (Vela), PSR J1119-6127 and PSR B1509-58. The braking index of a pulsar can be related to the slope of the track of that pulsar in the $P - \dot{P}$ ($\log P - \log \dot{P}$) plane:

$$d \log \dot{P} / d \log P = \ddot{P}P/\dot{P}^2 \equiv n' = 2 - n \quad (10)$$

The braking index is related to β and γ through the equation

$$n = 3 - 4/(1 + \beta\Omega^4/\gamma) \quad (11)$$

(Eq. 6 of Menou, Perna and Hernquist 2001b). For pulsars with measured braking indices Eqs. (9) and (16) can be solved for β and γ in terms of the observed n , P and \dot{P} values. We derived (\dot{M}, B_{\perp}) values (2.8×10^{16} gm/s, 7.1×10^{12} G) for the Crab pulsar, (1.5×10^{16} gm/s, 8.9×10^{12} G) for PSR B0540-69, (1.4×10^{15} gm/s, 5.2×10^{12} G) for the Vela pulsar, (2.8×10^{13} gm/s, 8×10^{13} G) for PSR J1119-6127, and (3.6×10^{14} gm/s, 3×10^{13} G) for PSR B1509-58.¹

3. The Distribution of Pulsars in the $P - \dot{P}$ Diagram

We used P and \dot{P} data from the Princeton Pulsar Catalog (Taylor et al. 1996). Tracks corresponding to Eq.(8) are shown in Fig 1. At early times (small P), the dipole term dominates and the pulsar follows the left branch of the track, which is essentially spin-down

¹The magnetic field of PSR J1119-6127 is $B_{\perp} = 8.2 \times 10^{13}$ G if one assumes dipole spin-down. Camilo et al (2000) report $B_{\perp} = 4.1 \times 10^{13}$ G in the discovery paper due to a missing factor of 1/2 in the definition of the neutron star's dipole moment.

under the magnetic dipole radiation torque, at constant magnetic field. The braking index for pure dipole spin-down is $n=3$, and the left branch of each track follows the slope $n' = -1$ in the $\log \dot{P} - \log P$ diagram,

$$P\dot{P} = (4\pi^2\beta/I) \propto B_{\perp}^2. \quad (12)$$

The transition to the regime in which the propeller torque dominates occurs at the minimum of a track, at the period

$$P_0 = (2\pi)(\beta/3\gamma)^{1/4} = 2\pi/\Omega_0. \quad (13)$$

The slope $n' = 0$, and the corresponding braking index $n = 2$ at this point. The minimum value of the spin-down rate is found to be

$$\dot{P}_{min} = (4\pi^2\beta/I)P_0^{-1} + (\gamma/4\pi^2I)P_0^3 = (8\pi/I)\gamma^{1/4}(\beta/3)^{3/4}. \quad (14)$$

The propeller spin-down torque is dominant along the right branch of each track. The asymptotic behaviour, reached already at periods of about $2P_0$, has the slope $n' = 3$ corresponding to a braking index $n = -1$. The evolution is very rapid on this branch. Neutron stars will spin-down to $\Omega = 0$ ($P = \infty$) in a finite time:

$$t_{max} = \pi\tau/2 = 7 \times 10^7 \dot{M}_{10}^{-1/2} B_{\perp,12}^{-1} \text{ yrs.} \quad (15)$$

A third of this time is spent until reaching the minimum \dot{P} at $P = \dot{P}_0$. About $0.23t_{max}$ is spent until reaching $n = 2.5$, $P = (3/7)^{1/4} \cong 0.8P_0$, when the pulsar has started deviating from dipole spin-down. The evolution slows down at periods around the turning point at P_0 to $P = \sqrt{3}P_0$, $n = 0$. From $n = 2.5$, $P \cong 0.8P_0$ to $P = \sqrt{3}P_0$, $n = 0$ it takes $0.44t_{max}$. As the pulsar proceeds into the propeller spin-down branch, the evolution speeds up, as $\dot{P} \propto P^3$; spin-down from $P = \sqrt{3}P_0$ to $P = \infty$ takes only $t_{max}/3$.

Pulsar activity will turn off at reaching a critical voltage (the "death lines", "the death valley") at a period satisfying $B_{\perp,12}/P^2 = \alpha = 0.1 - 1$ (see Fig 1). The propeller spin-down tracks are parallel to the death lines. In our analysis of the $P - \dot{P}$ diagram we find that the minimum mass inflow rate for the pulsars in our sample is $\dot{M}_{min} = 4.5 \times 10^8 \text{ gm s}^{-1}$. The propeller spin-down track for \dot{M}_{min} bounds the pulsar population on the right and is of the form $B_{\perp,12}/P^2 = 0.3$. This track is already in the death valley. Pulsars with $\dot{M} < \dot{M}_{min}$ will reach the death valley and turn off while they are still on the dipole spin-down track. Pulsars with $\dot{M} > \dot{M}_{min}$ will evolve on their propeller spin-down tracks until they reach $P_{death} = (B_{\perp,12}/\alpha)^{1/2}$ at an age

$$t_{death} = t_{max}[1 - (2/\pi) \arctan(0.7\alpha(\dot{M}_{10})^{-1/2})]. \quad (16)$$

This age for pulsar turnoff is close to t_{max} for almost all cases. Even for the track at \dot{M}_{min} with $\alpha = 0.3$ we find $t_{death} = 0.5t_{max}$. At times close to t_{max} evolution is rapid. Few

pulsars are observed at late times (long periods) along the propeller spin-down tracks as our histograms below confirm. Therefore pulsar turnoff will not effect the distribution of pulsars in the $P - \dot{P}$ diagram except for the lowest \dot{M} .

The spindown lifetime t_{max} is plausible in view of the low \dot{M} values obtained for the pulsar tracks. A time dependent disk would reach $\dot{M} = 10^8 - 10^{10}$ gm s⁻¹ on timescales $\sim 10^7 - 10^8$ yrs. If the disk is depleted before the pulsar completes its evolution the pulsar will switch to the pure dipole spin-down track corresponding to its magnetic field, at the same period it had on the propeller spin-down track, but at a much lower \dot{P} . The new position corresponds to propeller spin-down tracks of lower \dot{M} and is closer to or beyond the death lines.

The number ΔN of pulsars with magnetic field B_{\perp} and mass inflow rate \dot{M} in a period interval ΔP at period P is

$$\begin{aligned}\Delta N &= (\Delta N(P; \beta, \gamma)/\Delta P)\Delta P = Rf(P, \dot{P})(\Delta t(P; \beta, \gamma)/\Delta P)\Delta P \\ &= Rf(P, \dot{P})(\dot{P}(P; \beta, \gamma))^{-1}\Delta P\end{aligned}\quad (17)$$

Here R is the birthrate of pulsars in the galaxy, and $f(P, \dot{P})$, the fraction of the galactic disk volume in which pulsars of period P and period derivative \dot{P} are observable, describes selection effects. For simplicity we take $f(P, \dot{P})$ to be constant, assuming that the variation in $f(P, \dot{P})$ is negligible compared to the variation of \dot{P} . We further assume that one and only one track (β, γ) passes through each point in the $P - \dot{P}$ plane, such that the plane can be divided into strips separated by chosen (β, γ) tracks. For each strip we count the pulsars in equal sized period bins and construct the histogram of ΔN . We then choose a representative track $(\bar{\beta}, \bar{\gamma})$ for the strip such that the function $\Delta N(P) = \text{constant}/\dot{P}(P; \bar{\beta}, \bar{\gamma})$ matches the histogram.

The combined dipole and propeller spin-down model has a minimum \dot{P} at the turnover period P_0 on each track. $\Delta N \propto \dot{P}^{-1}$ must have a maximum at P_0 ; the largest number of pulsars are observed near P_0 since this is where their motion across the $P - \dot{P}$ diagram is slowest. The model predicts that $\Delta N \propto \dot{P}^{-1}$ will increase in proportion to P at short periods, and decrease in proportion to P^{-3} at $P > P_0$. The histograms do have this property. For each strip, we fit the histogram by choosing $\bar{\beta}$ to have the average value for the strip and choosing $\bar{\gamma}$ such that P_0 is in the period bin with the maximum number ΔN_{max} of pulsars. The normalization of the model curve is chosen to match the histogram at $(P_0, \Delta N_{max})$. Four strips separated by tracks with $B_{\perp,12} = 50, 4, 2, 0.8$ and 0.1 are shown on the $P - \dot{P}$ diagram in Fig.1. For the upper four tracks $P_0 = 0.3$ s, and for the lowest track at $B_{\perp,12} = 0.1$, $P_0 = 0.8$ s.

4. Results and Discussion

Our results show that the number distribution of pulsars in the $P - \dot{P}$ plane is fitted remarkably well with the combined effect of dipole and propeller spin-down. The mass inflow rates range from a few 10^{16} gm/s for the youngest pulsars to a minimum of 4.5×10^8 gm/s. The histograms for the four strips shown in Fig.2 show reasonable agreement with representative model curves. The agreement with the model is not sensitive to the choice of strip boundaries except for $B_{\perp,12} < 0.4$ where a second peak appears in the histograms at $P \simeq 1.3$ s. This also contributes to the histogram for $0.1 < B_{\perp,12} < 0.8$ in Fig.2d. This excess may reflect disk depletion resulting in pulsars dropping down, from many propeller spin-down tracks at higher B_{\perp} and \dot{M} , to their corresponding pure dipole spin-down tracks at periods close to death lines; the new positions where the excess is produced correspond to lower \dot{M} values on propeller spin-down tracks.

This result was obtained with an analytic model ignoring selection effects. Work is in progress to produce a Monte-Carlo simulation of the $P - \dot{P}$ diagram with the combined effects of dipole and propeller spin-down. Independent random distributions of B and \dot{M} are incorporated in the Monte-Carlo simulation, so that more than one track can go through a given point and there can be points not reached by any tracks in the $P - \dot{P}$ diagram, even in parts where observed pulsars cluster.

The time dependence of the disk and the mass inflow rate it supplies could also be incorporated in a more detailed calculation. The self similar isolated thin disk models with a power law decay of $\dot{M}(t)$ were employed by Menou, Perna and Hernquist (2001b) who point out that for the Crab pulsar, PSR B0540-09 and PSR B1509-58, thin disks in the \dot{M} ranges indicated by the braking indices of these pulsars are consistent with observational constraints in the optical though most of the disk luminosity would be in the UV where detections are much harder. For the Vela pulsar only a very small and highly inclined disk could be compatible with observational constraints. Menou, Perna and Hernquist (2001a) have shown that the thin disks may become neutral and stop evolving as thin disks. The transition will also quench the disk's luminosity. The application here to all pulsars across the $P - \dot{P}$ diagram and its success in fitting the pulsar distribution require and support the presence of low mass, low \dot{M} disks, which are active for pulsar lifetimes of the order of 10^7 yrs and remain attached to the light cylinder. According to the classification of Alpar (2001) disks are present around all classes of young neutron stars, providing accretion for AXPs and RQNSs, and acting as propellers on DTNs. For two AXPs and the RQNS in Cas A luminosities predicted by thin disk models are ruled out or tightly constrained by observations in the optical and IR (Coe & Pightling 1998, Hulleman et al 2000, Hulleman, van Kerkwijk & Kulkarni 2000, Kaplan, Kulkarni & Murray 2001). It is likely that disks

under propeller boundary conditions are not standard thin disks (Alpar 2001). As the mass inflow is stopped at the disk-magnetosphere boundary and largely ejected from the system, the disk may be enshrined in a corona and outflow of ejected matter, possibly with larger effective area and softer spectrum. The present application to the $P - \dot{P}$ diagram shows no indication of an effect on the pulsar distribution due to depletion of the disk before pulsar turnoff, except possibly for the oldest pulsars, well advanced in their evolution on propeller spin-down tracks, dropping down to pure dipole tracks near death lines as we discussed above. This may indicate that there is no separate disk timescale. Disks interacting with pulsars via propeller torques may be driven by these torques to evolve on the propeller spin-down timescales of the pulsars. These problems, as well as the assumption that the disk remains attached to the light cylinder require further work on the coupling between the disk and the pulsar magnetosphere.

We predict that some pulsars have braking indices < 2 , like the Vela pulsar (though the $n = 1.4 \pm 0.2$ braking index measurement for this pulsar should be treated with some caution as its timing behaviour is dominated by interglitch relaxation). About 2/3 of all pulsars will be on the propeller spin-down branch, with $n < 2$, at $P > P_0$. Half of these pulsars will have negative braking indices, $-1 < n < 0$. Measurement of braking indices is unfortunately very difficult since the timing behaviour is dominated by noise (Baykal et al 1999) and it seems also by interglitch recovery (Alpar and Baykal 2001).

The model also predicts very small numbers $\Delta N \propto P^{-3}$ of long period pulsars with large \dot{P} values. These pulsars would give magnetic fields $B_\perp \sim 10^{12} - 10^{13}$, perhaps 10^{14} G with the combined dipole-propeller spin-down model. For these pulsars the pure dipole spin-down model would yield higher fields, extending into the magnetar range. Propeller spin-down would also increase the rate of energy dissipation in pulsars and in neutron stars evolving under propeller torques after pulsar activity is over.

We thank O. H. Guseinov and Ü. Ertan for discussions and S. Ç. İnam for technical support. We thank TÜBİTAK, the Scientific and Technical Research Council of Turkey, for support through TBAG-ÇG4 and through the BDP program for doctoral research. AA & EY thank TÜBİTAK for graduate student scholarships. MAA thanks the Turkish Academy of Sciences and Sabancı University for research support.

REFERENCES

Alpar, M.A. 1999, <http://xxx.lanl.gov/abs/astro-ph/9912228>
Alpar, M.A. 2001, <http://xxx.lanl.gov/abs/astro-ph/0005211>, ApJ, in the press
Alpar, M.A. & Baykal, A. 2001, to be submitted
Baykal, A., Alpar, M.A., Boynton, P.E. & Deeter, J.E. 1999, MNRAS, 306, 207
Camilo, F. et al. 2000, ApJ, 541, 367
Canizzo, J.K., Lee, H.M. & Goodman, J. 1990, ApJ, 351, 38
Chakrabarty, D. et al. 2001, ApJ, 548, 800
Chatterjee, P., Hernquist, L. & Narayan, R. 2000, ApJ, 534, 373
Coe, M.J. & Pightling, S.L. 1998, MNRAS, 299, 233
Gaensler, B.M. & Frail, D.A. 2000, Nature, 406, 158
Gvaramadze, V.V. 2001, <http://xxx.lanl.gov/abs/astro-ph/0102431>
Hulleman, F., van Kerkwijk, M.H., Verbunt, F.W.M. & Kulkarni, S.R. 2000, A&A, 358, 605
Hulleman, F., van Kerkwijk, M.H. & Kulkarni, S.R. 2000, Nature, 408, 689
Illarionov, A.F. & Sunyaev, R.A. 1975, A&A, 39, 185
Kaplan, D.L., Kulkarni, S.R. & Murray, S.S. 2001, <http://xxx.lanl.gov/abs/astro-ph/0102054>
Marsden, D., Lingenfelter, R.E. & Rothschild, R.E. 2001a, ApJ 547, L45
Marsden, D., Lingenfelter, R.E. & Rothschild, R.E. 2001b, <http://xxx.lanl.gov/abs/astro-ph/0102049>
Menou, K., Perna, R. & Hernquist, L. 2001a, <http://xxx.lanl.gov/abs/astro-ph/0102478>
Menou, K., Perna, R. & Hernquist, L. 2001b, <http://xxx.lanl.gov/abs/astro-ph/0103326>
Mereghetti, S. 1999, to appear in The Neutron Star - Blackhole Connection, C. Kouveliotou, J. van Paradijs & J. Ventura, eds, (Kluwer: Dordrecht), <http://xxx.lanl.gov/abs/astro-ph/9911252>
Michel, F.C. 1988, Nature, 333, 644
Michel, F.C. & Dessler, A.J. 1981, ApJ, 251, 654
Michel, F.C. & Dessler, A.J. 1983, Nature, 303, 48
Mineshige, S., Nomoto, K. & Shigeyama, T. 1993, A&A, 267, 95
Taylor, J.H., Manchester, R.N. & Lyne, A.G., 1996, The Princeton Pulsar Catalog, <http://pulsar.ucolick.org/cog/pulsars/catalog>
Thompson, C. & Duncan, R.C. 1995, MNRAS 275, 255
Treves, A. et al. 2000, PASP, 112, 297
Woods, P.M. et al. 1999, ApJ 519, L139
Yusifov, I.M., Alpar, M.A., Gök, F., & Guseinov, O.H. 1995, M.A. Alpar, U. Kiziloglu, J. van Paradijs (eds.) The Lives of the Neutron Stars, P.201, Dordrecht: Kluwer.

Figure Captions

Figure 1. The $\log P(\text{s}) - \log \dot{P}$ (s s^{-1}) diagram. Strips used for the histograms in Fig.2 are separated by the tracks shown, $B_{\perp,12} = 50 - 4$ (Fig.2a), $B_{\perp,12} = 4 - 2$ (Fig.2b), $B_{\perp,12} = 2 - 0.8$ (Fig.2c), and $B_{\perp,12} = 0.8 - 0.1$ (Fig.2d). The dashed lines are death lines $B_{\perp,12}/P^2 = \alpha$ for $\alpha = 1, 0.3$ and 0.1 (left to right).

Figure 2. Histograms showing the number of pulsars in period bins for each of the strips shown in Fig.1. The model curve on each histogram is drawn for the average $\beta \propto B_{\perp,12}^2$ for the strip, with $\gamma \propto \dot{M}$ chosen such that the maximum of the histogram occurs at $P_0 = 2\pi(\beta/3\gamma)^{1/4}$.

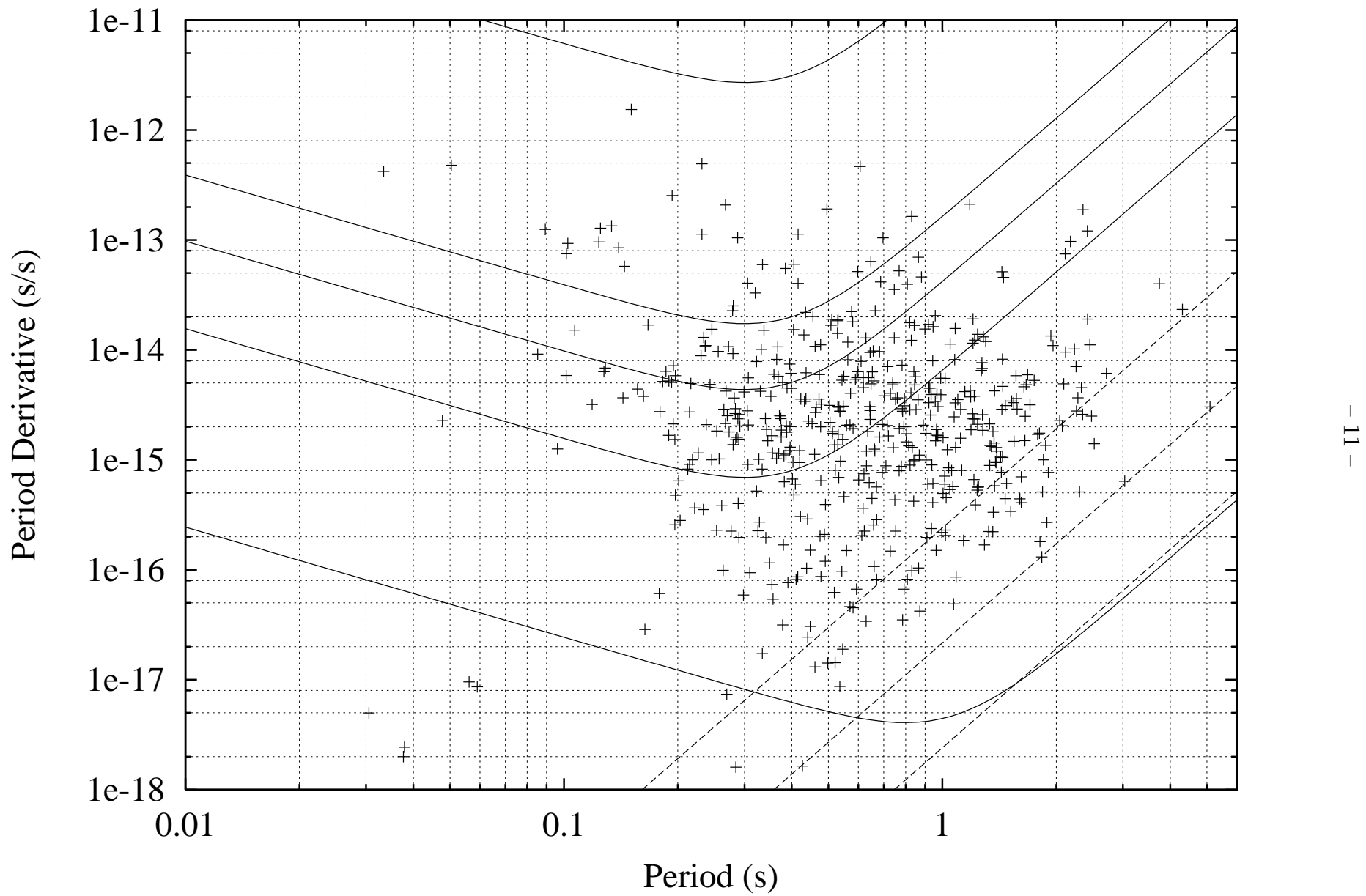
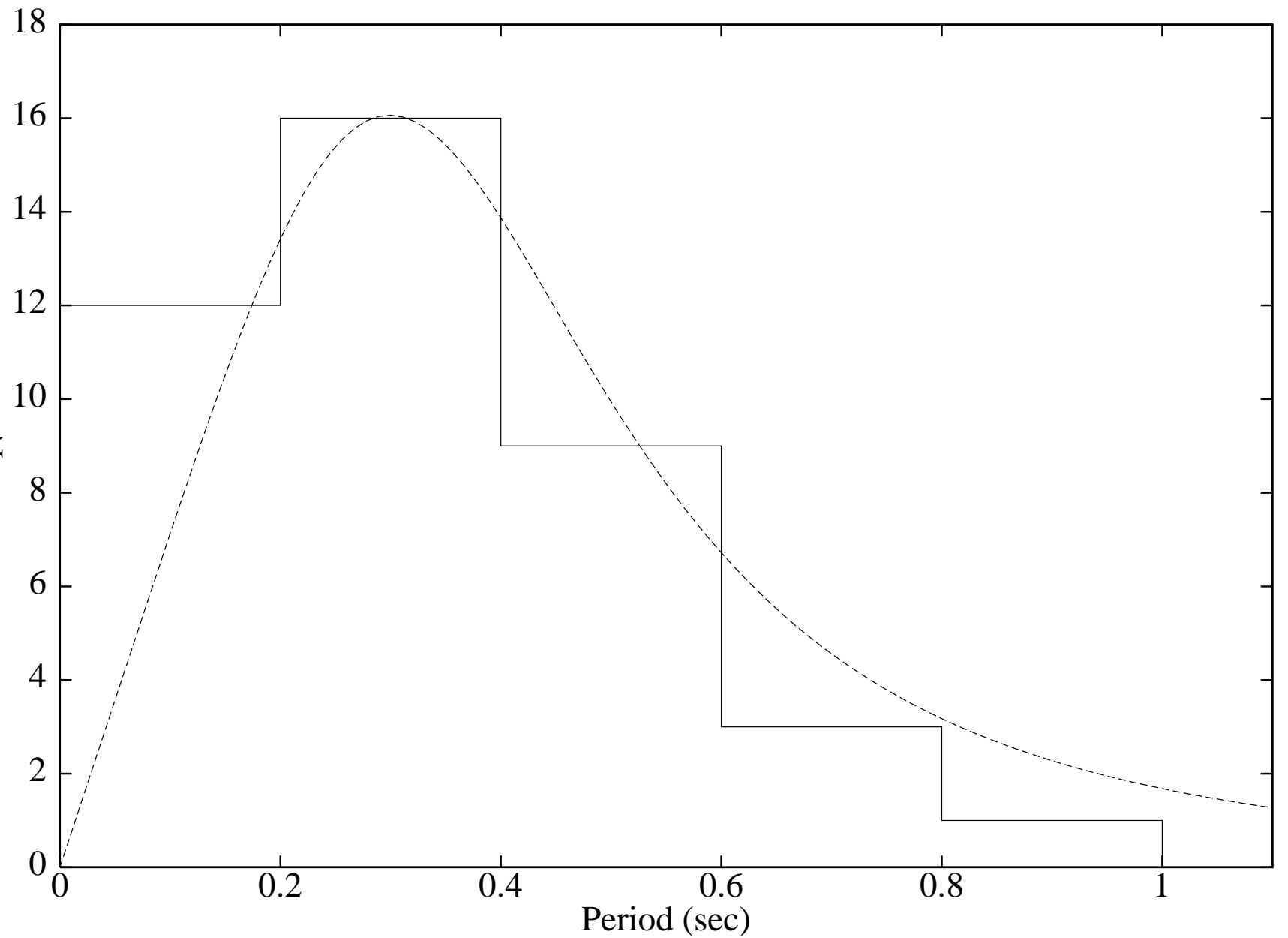


Fig.2a



- 12 -

